Thermochimica Acta, 204 (1992) 45–54
Elsevier Science Publishers B.V., Amsterdam

Relationships between the liquidus temperature and the formation of quasicrystalline phases in rapidly solidified Al–Cu–Mn alloys [1]

S. Maâmar, F. Faudot and M. Harmelin

CNRS–Centre d'Études de Chimie Métallurgique, 15, rue Georges Urbain, F-94407 Vitry-sur-Seine Cedex (France)

(Received 30 August 1991; in final form 9 December 1991)

Abstract

The alloys $Al_{75}Cu_{10}Mn_{15}$ (T_1), $Al_{57}Cu_{32.5}Mn_{10.5}$ (T_2) and $Al_{65}Cu_{20}Mn_{15}$ were prepared by rapid solidification from the melt. The flakes thus obtained were investigated by means of differential thermal analysis (DTA), X-ray diffraction (XRD) and transmission electron microscopy (TEM) in the as-quenched state and after annealing. The occurrence of icosahedral (i) and decagonal (d) quasicrystalline phases was observed in the as-quenched alloys. The i and d phases are both metastable and transform on heating into crystalline phases. The nature of the as-formed crystalline phases has been identified and found to be in agreement with those expected from the equilibrium phase diagram. For a heating rate of 10°C min^{-1}, the d phase begins to be decomposed above 600°C and the i phase above 400°C; the d phase is therefore more stable than the icosahedral phase. The liquidus temperatures of each alloy were determined by DTA on heating. By assuming that the undercooling interval is the same for each alloy during the quench, it is shown that the formation of the i or d phase is related to the respective liquidus temperatures of each alloy.

INTRODUCTION

Phase equilibria in the Al–Cu–Mn system have been investigated in detail by Köster and Gödecke [1], and an assessment of the complete equilibrium phase diagram was recently published [2]. In the Al-rich side, two intermetallic ternary phases T_1 and T_2 and a bcc ternary solid solution β are reported to exist at room temperature.

According to ref. 1, the composition range of T_1 is given around $Al_{72}Cu_{10}Mn_{18}$ (the subscripts represent nominal atomic percentages of the

Correspondence to: S. Maâmar, CNRS–Centre d'Etudes de Chimie Métallurgique, 15, rue Georges Urbain, F-94407 Vitry-sur-Seine Cedex, France.

[1] This paper was presented during the 22nd annual meeting of the French Association of Calorimetry and Thermal Analysis (AFCAT) at Paris-XI–Châtenay-Malabry (27–29 May 1991).

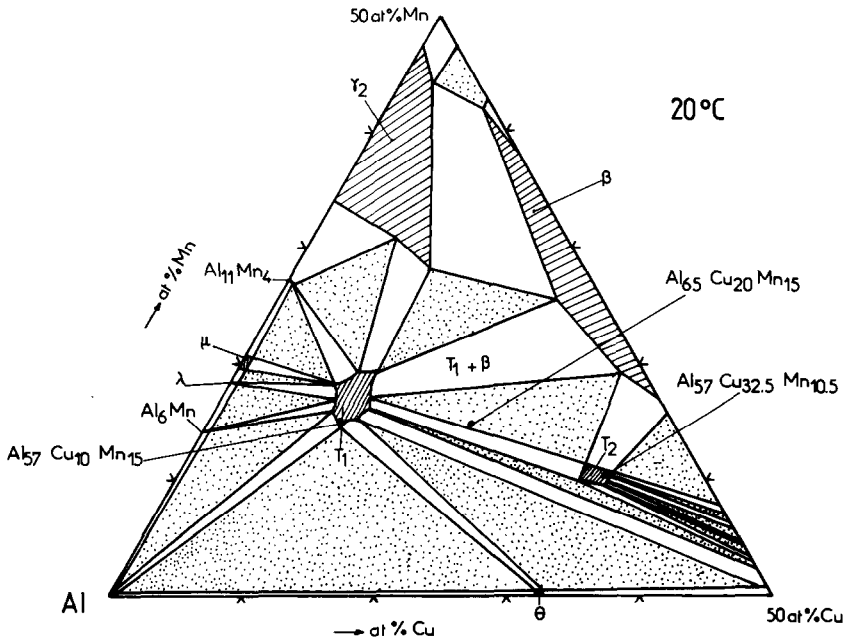

Fig. 1. Isothermal section at room temperature in the Al-rich side showing the composition points (filled circles) of the three alloys investigated in this work: $Al_{75}Cu_{10}Mn_{15}$ (T_1), $Al_{57}Cu_{32.5}Mn_{10.5}$ (T_2) and $Al_{65}Cu_{20}Mn_{15}$. On this figure, we have chosen the single phase domain proposed by Köster and Gödecke for T_1 [1].

respective components) but the structure was left unidentified. However, Robinson [3] has shown that the compound $Cu_2Mn_3Al_{20}$ (i.e. $Al_{80}Cu_8Mn_{12}$ following our formula representation given above) has an orthorhombic structure (oC156, $a = 2420$, $b = 1250$ and $c = 772$ pm) similar to that of $Ni_4Mn_{11}Al_{60}$. The crystal structure of $Ni_4Mn_{11}Al_{60}$ was described by Robinson [4] as a layered structure. A considerable variation of composition was reported in [3] for $Cu_2Mn_3Al_{20}$, and it can be therefore expected that T_1 and $Cu_2Mn_3Al_{20}$ are the same phases. T_1 is reported to melt congruently at 1020°C in [1].

The T_2 phase was first reported by Guertler and Rassmann [5] and given as $Mn_3Cu_5Al_{11}$ ($Al_{58}Cu_{26}Mn_{16}$). Later on, Köster and Gödecke [1] showed that T_2 is formed at 700°C by a peritectoid reaction between β and T_1 and has an orthorhombic structure (oP380, $a = 1210$, $b = 2408$, $c = 1921$ pm) with a small range of homogeneity around the $Al_{57}Cu_{32}Mn_{11}$ composition. In this paper, the composition $Al_{57}Cu_{32.5}Mn_{10.5}$ was used for T_2.

The isothermal section at room temperature in the Al-rich part (up to 50 at% of Mn and 50 at% of Cu) of the Al–Cu–Mn phase diagram is shown in Fig. 1. We have drawn the respective existence fields of the various phases by combining the recent Al–Mn [6] and Al–Cu [7] assessed binary diagrams with the ternary equilibrium phase diagram reported by Köster

and Gödecke [1]. The location of the three alloy compositions investigated in this paper ($Al_{75}Cu_{10}Mn_{15}$ (T_1), $Al_{57}Cu_{32.5}Mn_{10.5}$ (T_2) and $Al_{65}Cu_{20}Mn_{15}$) is shown as filled circles.

The composition $Al_{65}Cu_{20}Mn_{15}$ was used in this work for investigating the formation of the quasicrystalline phases. This is the composition for which the icosahedral (i) quasicristalline phase was first observed by Tsai et al. [8]. These authors prepared the i phase by melt spinning. They found that i was not stable because it exhibited an exothermic peak on heating in a differential scanning calorimeter (DSC). The exothermic phenomenon was interpreted by Tsai et al. as the transformation of the quasicrystal to a crystalline structure. No attempt was made to identify the nature of the as-formed periodic crystal(s). The metastability of the i phase was confirmed for the same alloy composition by Ebalard and Spaepen [9]. These authors also used melt spinning for obtaining the i phase; moreover, when the alloys were melt spun at low speed they observed the occurrence of the decagonal (d) phase.

We have shown in a recent paper [10] the existence of a hierarchy of stability between the i and d phases, essentially based on X-ray diffraction results. In the present paper, we discuss in more detail the formation and the origin of the i and d quasicrystalline phases in relation to the liquidus temperatures of the alloys.

EXPERIMENTAL PROCEDURE

Three compositions of alloys were investigated: $Al_{75}Cu_{10}Mn_{15}$ (T_1), $Al_{57}Cu_{32.5}Mn_{10.5}$ (T_2) and $Al_{65}Cu_{20}Mn_{15}$ (Fig. 1).

The master ingots were prepared under a controlled helium atmosphere by induction melting of the commercial pure elements (Al 6N, Cu Asarco 5N, Mn 4N). Each entire ingot was then rapidly quenched by planar flow casting, and small flakes of about 30 μm thickness and some mm^2 area were obtained.

A SETARAM micro differential thermal analyser (DTA) was used to determine the thermal stability of the different alloys. The specimens (typically 20 mg) were put inside alumina crucibles and heated at 10°C min^{-1} in flowing pure argon up to 1100°C.

X-ray diffraction (XRD) and transmission electron microscopy (TEM) were used to establish the structures of the various phases [10].

RESULTS AND INTERPRETATION

Solid state reactions on annealing the as-quenched alloys

The DTA curves obtained on heating the as-quenched flakes up to 700°C for $Al_{75}Cu_{10}Mn_{15}$ (Fig. 2), 650°C (Fig. 3) for $Al_{57}Cu_{32.5}Mn_{10.5}$ (which

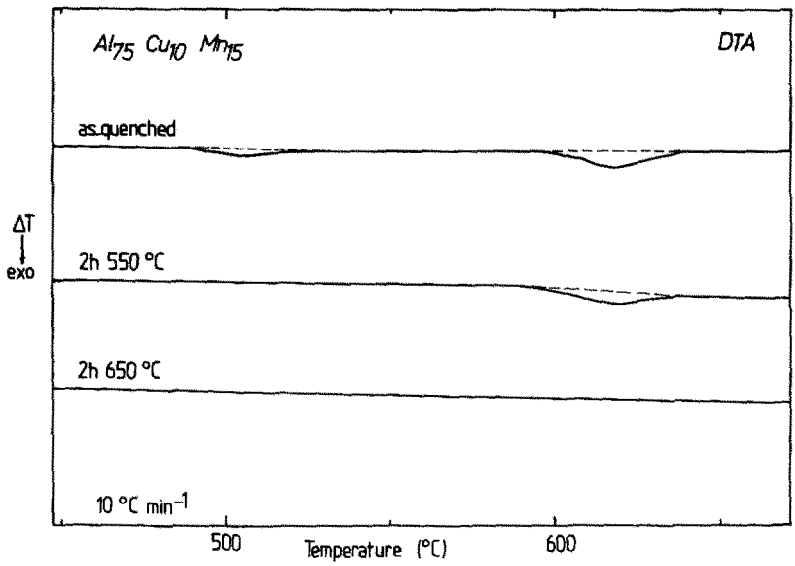

Fig. 2. DTA curves obtained with $Al_{75}Cu_{10}Mn_{15}$ in the as-quenched state and after annealing for 2 h at 550 or 650°C.

begins to decompose at 680°C) and 700°C (Fig. 4) for $Al_{65}Cu_{20}Mn_{15}$ show exothermic phenomena during the first heating of the flakes (solid curves). These effects are irreversible because they are no longer observed when

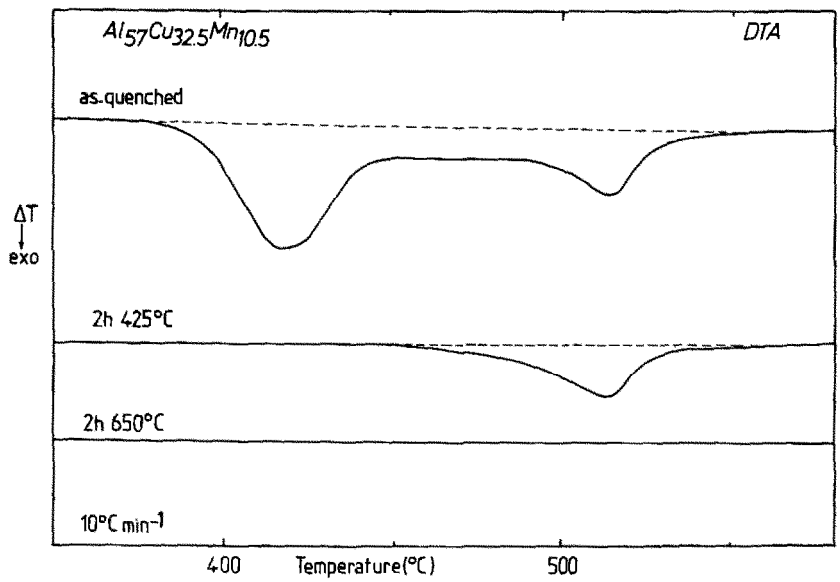

Fig. 3. DTA curves obtained with $Al_{57}Cu_{32.5}Mn_{10.5}$ in the as-quenched state and after annealing for 2 h at 425 or 650°C.

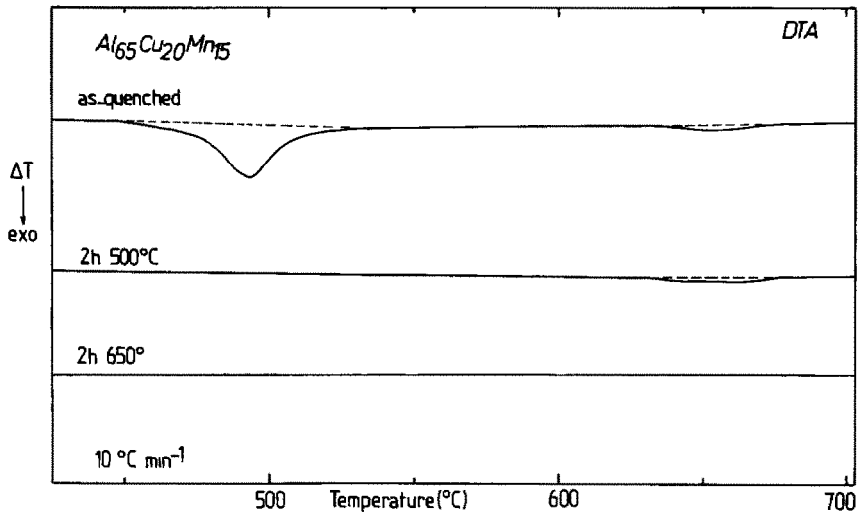

Fig. 4. DTA curves obtained with $Al_{65}Cu_{20}Mn_{15}$ in the as-quenched state and after annealing for 2 h at 500 or 650°C.

the same specimens are heated a second time after cooling to room temperature (dotted curves).

The phase transformations at the origin of these effects were investigated by annealing the alloys for 2 h at 550°C for $Al_{75}Cu_{10}Mn_{15}$, 425°C for $Al_{57}Cu_{32.5}Mn_{10.5}$ and 500°C for $Al_{65}Cu_{20}Mn_{15}$, and also at 650°C for the three compositions. The effect of these annealing treatments on the corresponding DTA curves are shown in Fig. 2 for $Al_{75}Cu_{10}Mn_{15}$, Fig. 3 for $Al_{57}Cu_{32.5}Mn_{10.5}$ and Fig. 4 for $Al_{65}Cu_{20}Mn_{15}$. The nature and the structure of the phases determined by XRD and TEM in the as-quenched flakes and after annealing and cooling to room temperature are summarized in Table 1.

From these results, the exothermic peaks observed on the DTA curves are interpreted as follows.

For $Al_{75}Cu_{10}Mn_{15}$ (Fig. 2), the weak exothermic peak around 500°C results from the disappearance of θ-Al_2Cu, as expected for this alloy composition in this side of the equilibrium phase diagram, and of the traces of the i phase. The second peak around 600°C is explained by the transformation from the d phase to the periodic T_1 phase.

For $Al_{57}Cu_{32.5}Mn_{10.5}$ (Fig. 3), the first and broad exothermic peak around 425°C results from various simultaneous reactions: transformation of the i phase into the d phase and beginning of the formation of the T_2 phase by reaction between β and the d phase (corresponding to T_1). The complete formation of T_2 is revealed by the second peak around 525°C.

For $Al_{65}Cu_{20}Mn_{15}$ (Fig. 4), the first exothermic peak between 450 and 520°C also results from various simultaneous reactions: transformation of

TABLE 1

Various phases identified by XRD and TEM in the as-quenched flakes and after annealing. First anneal: 2 h at 425°C ($Al_{57}Cu_{32.5}Mn_{10.5}$), 500°C ($Al_{65}Cu_{20}Mn_{15}$) or 550°C ($Al_{75}Cu_{10}Mn_{15}$). Second anneal: 2 h at 650°C

Heat treatment	$Al_{75}Cu_{10}Mn_{15}$	$Al_{57}Cu_{32.5}Mn_{10.5}$	$Al_{65}Cu_{20}Mn_{15}$
As-quenched	i?	i	i
	d	d	d
	Al_2Cu	–	–
	–	β	β
After the first anneal	d	d	d
	–	β [a]	β [a]
		T_2?	T_2?
After the second anneal	–	β?	β?
	T_1	T_2	T_1+T_2

Key: i, icosahedral structure; d, decagonal structure; ?, traces. T_1 and T_2 are orthorhombic structure.

[a] Note that the XRD peak intensity of the β phase is decreased after the first annealing.

the i phase into the d phase and beginning of the formation of the T_2 phase by solid state reaction between β and the d phase (T_1 composition). The second peak above 620°C results from the transformation of the residual d phase into the T_1 periodic phase.

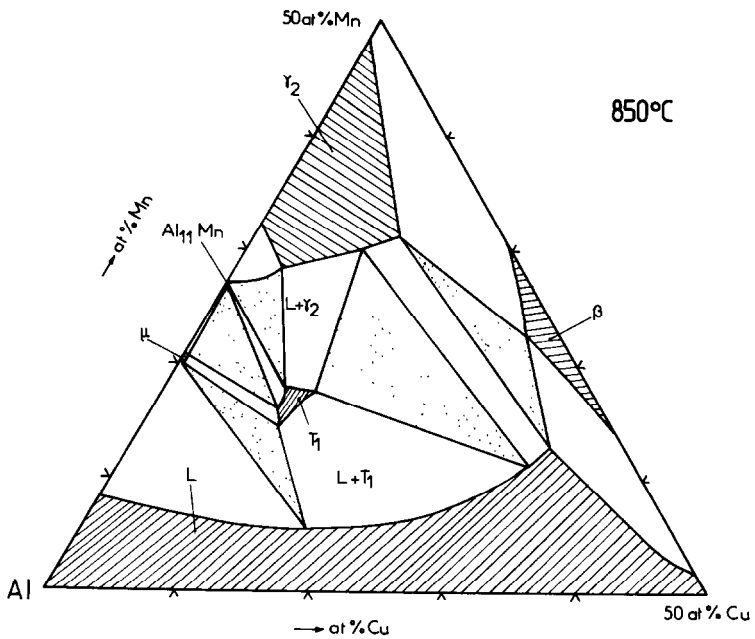

Fig. 5. Isothermal section of the Al–Cu–Mn system at 850°C.

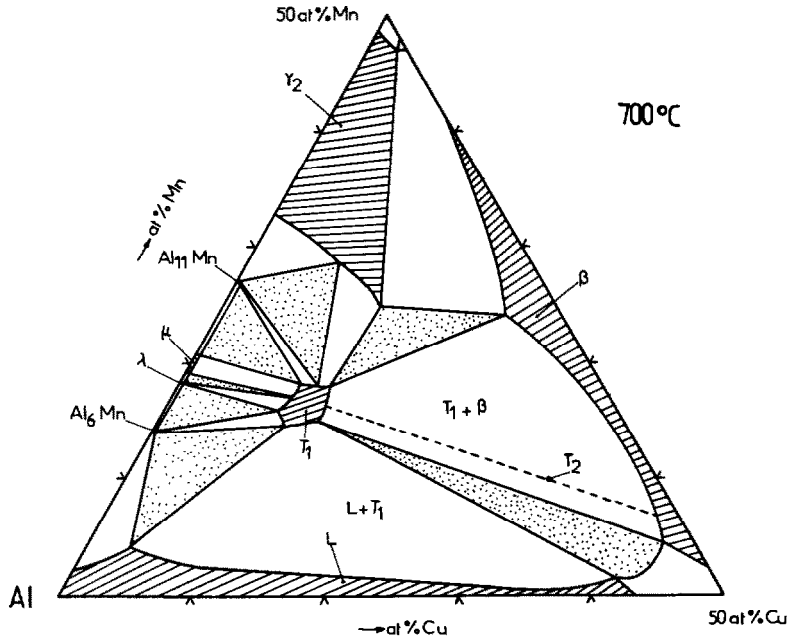

Fig. 6. Isothermal section of the Al–Cu–Mn system at 700°C (the tie line between T_1 and β corresponding to the peritectoid formation of T_2 is shown).

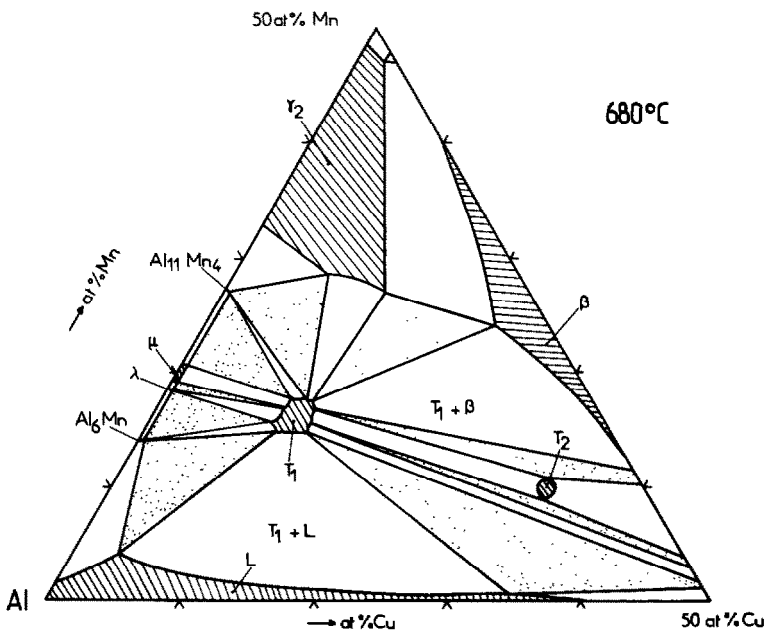

Fig. 7. Isothermal section of the Al–Cu–Mn system at 680°C.

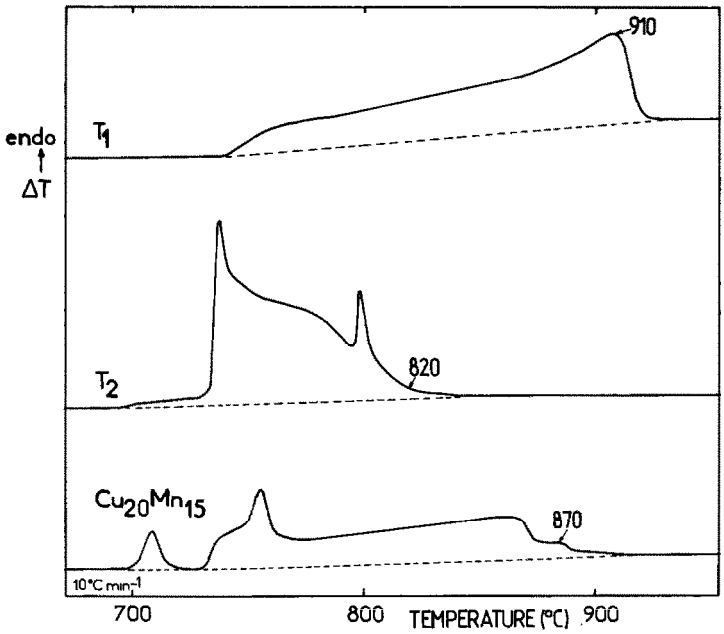

Fig. 8. DTA curves obtained with T_1 ($Al_{75}Cu_{10}Mn_{15}$), T_2 ($Al_{57}Cu_{32.5}Mn_{10.5}$) and $Al_{65}Cu_{20}Mn_{15}$ in the melting temperature range.

The phase transformations at the origin of T_2 are illustrated in Figs. 5, 6 and 7. At 850°C and 700°C (Figs. 5 and 6), the T_1 crystalline phase and the ternary β solid solution are the only ternary single phases coexisting in this composition range. At 700°C (Fig. 6), just before the formation of T_2, the tie line corresponding to the reaction between T_1 and β is indicated. At 680°C (Fig. 7), T_2 is formed as a single phase. The two and three-phase fields between T_1, T_2 and β have been drawn by referring to the experimental data reported in [1].

Melting behaviour of the alloys

The DTA curves obtained on heating the alloys to complete melting are shown in Fig. 8. For $Al_{75}Cu_{10}Mn_{15}$ (T_1), the liquidus temperature is measured at $\approx$ 910°C. For $Al_{57}Cu_{32.5}Mn_{10.5}$ (T_2) the liquidus temperature is $\approx$ 820°C and for $Al_{65}Cu_{20}Mn_{15}$ it is $\approx$ 870°C.

DISCUSSION

The main feature which is derived from the results described above is related to the respective stabilities of the i and d phases. From Table 1 it can be concluded that: (a) the d phase remains undecomposed up to a temperature higher than that for the i phase, and (b) the i phase is

transformed on heating into the d phase. This latter conclusion is obtained from the behaviour of both alloys $Al_{57}Cu_{32.5}Mn_{10.5}$ and $Al_{65}Cu_{20}Mn_{15}$. After annealing at 425 and 500°C respectively, no orthorhombic periodic phase is formed and the β volume fraction decreases. That means that i is not transformed into a periodic phase. Because the only remaining phase is d, we conclude that i can only be transformed into d. The temperatures of the transformations of the i and d phases are essentially heating rate dependent. For a heating rate of 10°C min^{-1}, the destruction of i begins at $\approx$ 400°C and that of the d phase at 600°C (Figs. 3 and 4). For higher heating rates, e.g. 40°C min^{-1}, these temperatures are shifted to 450 and 650°C respectively.

The hierarchy of stability between the icosahedral and decagonal phases is in agreement with the theoretical treatment proposed by Narasimhan and Ho [11], who predicted that the decagonal structure has a lower free energy than the icosahedral structure. This difference between the i and d thermal stabilities is basically the most important feature for analysing the mechanism of the i and d respective formations of i and d, during rapid solidification.

(a) During the quench, the liquid is undercooled to a certain temperature (T_s) at which solid phases appear. The nature of the solid phases which are formed when solidification begins could be expected to correspond with the equilibrium phases at the temperature T_s. However, this is not the case, because in the as-quenched samples the periodic phases T_1 and T_2 which exist below 700°C (see Figs 1, 6 and 7) are never observed: i or d (with some cc β phase, depending on the alloy composition) are the only phases detected.

(b) The value of the temperature T_s at which solidification begins determines the structure of the quasicrystalline phase which is formed: for $T_s > 450$°C (the conventional higher temperature limit chosen here for the transformation of i into d) the d phase will be produced and for $T_s < 450$°C the i phase will be formed.

(c) The undercooling interval ΔT_u ($\Delta T_u = T_{liquidus} - T_s$) is determined by the quenching rate. Because the liquidus temperature is fixed for each alloy composition for a given quenching rate, the value of T_s will be determined only by the liquidus temperature of the alloy if ΔT_u is constant. High values of the liquidus temperatures will correspond to high values of T_s.

This allows one to understand why the i phase is formed more easily than the d phase for higher quenching rates, as observed by Ebalard and Spaepen [9].

If we assume that the quench conditions are highly reproducible and the undercooling interval is constant for the three alloys investigated, the value of T_s can thus be related to the liquidus temperature of each alloy.

The existence of the i phase in the as-quenched $Al_{57}Cu_{32.5}Mn_{10.5}$ ($T_{liquidus}$ = 820°C) and $Al_{65}Cu_{20}Mn_{15}$ ($T_{liquidus}$ = 870°C) and not in

$Al_{75}Cu_{10}Mn_{15}$ ($T_{liquidus}$ = 910°C) is explained by the increasing value of the liquidus temperature. The increase from 870 to 910°C can be considered as critical because the undercooling would correspond to the value of T_s critical for the formation of i or d.

CONCLUSIONS

Assuming that the undercooling range is constant for the three compositions of alloys investigated in this work, a relationship is evident between the liquidus temperature and the nature of the quasicrystalline (i or d) phase formed on quenching. The formation of the d phase is explained as being favoured over the i phase during the quench when the undercooled liquid is frozen in a high temperature region, i.e. at a temperature higher than the temperature of the transformation of the i phase into the d phase: the lower the quenching rate, the higher is the freezing temperature of the liquid. This is the consequence of the hierarchy of stability between the i and d phases: the d phase being more stable than the i phase.

ACKNOWLEDGEMENTS

The authors are grateful to Dr Y. Calvayrac and Dr C. Colinet for useful suggestions for improving the manuscript. Dr A. Quivy and Dr J. Devaud-Rzepski are also thanked for their kind help with the X-ray diffraction and TEM measurements.

REFERENCES

1 W. Köster and T. Gödecke, Z. Metallkde, 57 (1966) 889.
2 H.L. Lukas, Aluminium–copper–manganese, in G. Petzow and G. Effenberg (Eds.), Ternary Alloys, Vol. 4, VCH, Weinheim, 1991, p. 567.
3 K. Robinson, Philos. Mag., 43 (1952) 775.
4 K. Robinson, Acta Crystallogr., 7 (1954) 494.
5 W. Guertler and G. Rassmann, Metallwirtschaft, 22 (1943) 65.
6 A.J. McAlister and J.L. Murray, Bull. Alloy Phase Diagrams, 8 (1987) 438.
7 J.L. Murray, Int. Met. Rev., 30 (1985) 211.
8 A.P. Tsai, A. Inoue and T. Masumoto, J. Mater. Sci. Lett., 7 (1988) 322.
9 S. Ebalard and F. Spaepen, J. Mater. Res., 5 (1990) 62.
10 S. Maâmar and M. Harmelin, Philos. Mag. Lett., 64 (1991) 343.
11 S. Narasimhan and T.L. Ho, Phys. Rev. B, 37 (1988) 800.